T H E U N I V E R S I T Y O F R E A D I N G

Numerical Modelling of Traffic on the M25 Motorway: Part II

by

Joanne Morgan

Numerical Analysis Report 3/2001

D E P A R T M E N T O F M A T H E M A T I C S

Numerical Modelling of Traffic on the M25 Motorway: Part II

Joanne V. Morgan
University of Reading
Department of Mathematics
Whiteknights, PO Box 220,
Reading, Berkshire.
RG6 6AX.
August 2001

Abstract

This report is a comparison of two two-equation models of traffic flow which are based on the ideas of fluid dynamics. It discretises both models using Roe decomposition and a second order scheme. The results are then compared with real data.

1 Introduction

This is an addition to a previous report [11] on the one-equation Lighthill-Whitham-Richards model [10], [14]. In this report we consider two-equation models, first the Payne-Whitham model [13], [17] and secondly the Aw-Rascle model [1]. We discuss the application of a number of schemes and compare the numerical results to real averaged data from the M25 motorway.

Section 2 describes the two two-equation models. In Section 3 we discuss the schemes used. Results are presented in Section 4 using the data from the M25 motorway as initial conditions and boundary data where required. Conclusions are made in Section 5 and Section 6 proposes further work.

2 The Models

In this paper we are considering two different models, the Payne-Whitham model and the Aw-Rascle Model. Both consist of systems of two equations.

2.1 Payne-Whitham Model

A two-equation model was proposed in the 1970's independently by Payne [13] and by Whitham [17], we shall refer to this as the PW model. The first equation is the conservation of mass equation as discussed in [11], i.e.

$$\frac{\partial \rho}{\partial t} + \frac{\partial f(\rho)}{\partial x} = 0 \tag{1}$$

with ρ representing the density of vehicles and the flux function $f(\rho) = \rho v$ where v is the velocity. In the one-equation model a particular form of $v(\rho)$ is assumed. In the two-equation models v and ρ are assumed to be independent and a second equation formed connecting them, as in a fluid model.

The second equation is derived from the Navier-Stokes equation of motion for a one-dimensional compressible flow, but with a pressure $p = C_o^2 \rho$ and a relaxation term. This gives

$$\frac{\partial v}{\partial t} + v\frac{\partial v}{\partial x} = -\frac{C_o^2}{\rho}\frac{\partial \rho}{\partial x} + \left(\frac{V(\rho) - v}{\tau}\right) + \frac{\mu}{\rho} v_{xx} \tag{2}$$

where C_o and τ are constants, and the velocity $V(\rho)$ is the 'maximal and out of danger' velocity meant to mimic drivers' behaviour. Kerner and Konhäuser [6], henceforth described as KK, describe $V(\rho)$ as being 'determined by the average balance between safety requirements and risk readiness of the driver as well as legal traffic regulations and road conditions'. As in the first report [11] there are many possible choices for the velocity function $V(\rho)$. In this report we consider a simplified version of the equations with no viscosity or relaxation terms (see later).

In order to rewrite the left hand side of (2) in conservative form, first we use the product rule

$$(\rho v)_t = \rho v_t + v \rho_t$$

and, substituting in for $v\rho_t$ after multiplying (1) by v, we have that

$$v(\rho v)_x + (\rho v)_t - \rho v_t = 0. \tag{3}$$

Substituting (3) into (2) multiplied by ρ gives

$$\rho v_t + \rho v v_x = -C_o^2 \rho_x + \rho \frac{(V(\rho) - v)}{\tau} + \mu v_{xx}$$

while substituting for ρv_t from (3) gives

$$v(\rho v)_x + (\rho v)_t + \rho v v_x = -C_o^2 \rho_x + \rho \frac{(V(\rho) - v)}{\tau} + \mu v_{xx}. \tag{4}$$

Again using the product rule on $(\rho v v)_x$, i.e.

$$(\rho v v)_x = (\rho v)_x v + (\rho v) v_x$$

and substituting in (4) for $(\rho v)_x v + (\rho v) v_x$ we obtain

$$\left(\frac{(\rho v)^2}{\rho}\right)_x + (\rho v)_t = -C_o^2 \rho_x + \rho \frac{(V(\rho) - v)}{\tau} + \mu v_{xx}.$$

Hence we obtain the second equation (2) with the left hand side in conservative form

$$(\rho v)_t + \left(\frac{(\rho v)^2}{\rho} + C_o^2 \rho\right)_x = \rho \frac{(V(\rho) - v)}{\tau} + \mu v_{xx}. \tag{5}$$

The source terms on the right hand side consist of a relaxation term and a viscosity term.

The two equation conservative model, (1) and (5), can conveniently be written in the vector form

$$\mathbf{u}_t + \mathbf{f}(\mathbf{u})_x = \mathbf{R} \tag{6}$$

where

$$\mathbf{u} = \begin{pmatrix} \rho \\ \rho v \end{pmatrix}, \mathbf{f}(\mathbf{u}) = \begin{pmatrix} \rho v \\ \frac{(\rho v)^2}{\rho} + C_o^2 \rho \end{pmatrix} \tag{7}$$

and

$$\mathbf{R} = \begin{pmatrix} 0 \\ \rho \frac{(V(\rho) - v)}{\tau} + \mu v_{xx} \end{pmatrix}.$$

Here we shall consider the situation where there is no viscosity or relaxation, i.e. $\mathbf{R} = \mathbf{0}$, hence the problem reduces to that of isothermal flow [9].

Referring to (6), with $\mathbf{u}$, $\mathbf{f}(\mathbf{u})$ given by (7), we can write the system as

$$\frac{\partial \mathbf{u}}{\partial t} + A(\mathbf{u}) \frac{\partial \mathbf{u}}{\partial x} = \mathbf{0}, \tag{8}$$

where the matrix $A(\mathbf{u})$ is given by

$$A(\mathbf{u}) = \frac{\partial \mathbf{f}}{\partial \mathbf{u}} = \begin{pmatrix} 0 & 1 \\ C_o^2 - \frac{(\rho v)^2}{\rho^2} & \frac{2\rho v}{\rho} \end{pmatrix} \tag{9}$$

We can then find the eigenvalues λ and corresponding eigenvectors $\mathbf{e}$ of A in order to diagonalise it. From

$$|A - \lambda I| = 0$$

$$(-\lambda)(2v - \lambda) - \left(C_o^2 - v^2\right) = 0$$

$$\lambda^2 - 2v\lambda - \left(C_o^2 - v^2\right) = 0$$

giving

$$\lambda_1 = v + C_o, \quad \lambda_2 = v - C_o. \tag{10}$$

To obtain the corresponding eigenvectors $\mathbf{e}_1$ and $\mathbf{e}_2$ we seek a vector $\mathbf{x}$ that satisfies

$$(A - \lambda I)\mathbf{x} = \mathbf{0}.$$

So for λ_1 we have

$$\begin{pmatrix} -v - C_o & 1 \\ C_o^2 - v^2 & v - C_o \end{pmatrix} \mathbf{x} = \mathbf{0}.$$

Choosing x_1 to be 1, we get $x_2 = v + C_o$, giving the eigenvector

$$\mathbf{e}_1 = \begin{pmatrix} 1 \\ v + C_o \end{pmatrix}. \tag{11}$$

Similarly for λ_2 we get

$$\mathbf{e}_2 = \begin{pmatrix} 1 \\ v - C_o \end{pmatrix}. \tag{12}$$

2.2 Aw-Rascle Model

A model by Aw and Rascle [1] that claims to be an improvement on the PW model has recently been proposed. They argue that other researchers have stuck too closely to fluid flow models and not allowed for significant differences between traffic and fluids, e.g. traffic is more concerned with the flow in front, rather than behind.

The model proposed by Aw and Rascle, henceforth known as AR, is

$$\frac{\partial \rho}{\partial t} + \frac{\partial (\rho v)}{\partial x} = 0$$

as in (1), together with a Lagrangian equation

$$\frac{\partial(v+p(\rho))}{\partial t}+v\frac{\partial(v+p(\rho))}{\partial x}=0 \tag{13}$$

where $p(\rho)$ is a smooth increasing pressure function. They suggest

$$p(\rho)=C_0^2\rho^\gamma \tag{14}$$

for the pressure where $\gamma>0$, and $C_0=1$.

Multiplying (1) by ρ and using the product rule

$$(\rho(v+P))_t=\rho(v+P)_t+(v+P)\rho_t,$$

$$(\rho v(v+P))_x=\rho v(v+P)_x+(v+P)(\rho v)_x,$$

we get

$$(\rho(v+P))_t-(v+P)\rho_t+(\rho v(v+P))_x-(v+P)(\rho v)_x=0. \tag{15}$$

Now, using (1), we can reduce the left hand side of (15) to

$$(\rho(v+P))_t+(\rho v(v+P))_x=0. \tag{16}$$

This is now in conservative form, where the conserved variable is $\rho(v+P)=y$, say. Hence, rewriting the AR system using the conserved variables ρ and y, equations (1) and (15) become

$$\begin{aligned}(\rho)_t+(y-\rho P)_x&=0,\\ (y)_t+\left(\frac{y^2}{\rho}-yP\right)_x&=0.\end{aligned} \tag{17}$$

In the vector notation of (6) this is

$$\mathbf{u}=\begin{pmatrix}\rho\\ y\end{pmatrix},\mathbf{f}(\mathbf{u})=\begin{pmatrix}y-\rho P\\ \frac{y^2}{\rho}-yP\end{pmatrix},\mathbf{R}=\mathbf{0}, \tag{18}$$

which can then be written in the form of (8), with

$$A(\mathbf{u})=\begin{pmatrix}-(\gamma+1)P & 1\\ -\frac{y^2}{\rho^2}-\frac{\gamma Py}{\rho} & \frac{2y}{\rho}-P\end{pmatrix} \tag{19}$$

whose eigenvalues and corresponding eigenvectors are

$$\lambda_1 = v, \quad \lambda_2 = v - \gamma P \tag{20}$$

and

$$\mathbf{e}_1 = \begin{pmatrix} 1 \\ v + (\gamma + 1)P \end{pmatrix}, \quad \mathbf{e}_2 = \begin{pmatrix} 1 \\ v + P \end{pmatrix}. \tag{21}$$

3 The Schemes

In this report we shall consider the first order Lax-Friedrichs scheme as well as decomposing the models and applying a second order TVD scheme with flux limiters.

3.1 The Lax-Friedrichs Scheme

For systems such as (18), Lax-Friedrichs scheme is given by

$$\mathbf{u}_j^{n+1} = \frac{1}{2}\left(\mathbf{u}_{j+1}^n + \mathbf{u}_{j-1}^n\right) - \frac{\Delta t}{2\Delta x}\left(\mathbf{f}_{j+1}^n - \mathbf{f}_{j-1}^n\right), \tag{22}$$

where j, n are the space and time step indices respectively.

The scheme is first order accurate. It is known to smooth out solutions excessively and have a *step* feature, but it is nonetheless useful for getting a rough idea of the behaviour of the system very cheaply. It is conservative and easy to apply.

3.2 Roe's Scheme

The idea behind Roe's scheme is to take a non-linear system of the form (8) and to linearise it by approximating the Jacobian matrix $A(\mathbf{u})$ using Roe averages. The resulting system can then be decomposed into its two component waves travelling at approximate speeds given by the eigenvalues of the averaged Jacobian matrix $\tilde{A}(\tilde{\mathbf{u}})$.

3.2.1 Roe Decomposition

Given any data $\mathbf{u}$ we can form differences $\Delta\mathbf{u}$. We can then find values for α_1 and α_2 such that

$$\Delta\mathbf{u} = \sum_{k=1}^{2} \alpha_k \mathbf{e}_k, \tag{23}$$

i.e. project it onto the eigenvectors.

For an infinitesimally small difference $\Delta\mathbf{u}$ and a corresponding small $\Delta\mathbf{f}$, using (19),

$$\Delta\mathbf{f} = A(\mathbf{u})\Delta\mathbf{u} = \sum_{k=1}^{2} \lambda_k \alpha_k \mathbf{e}_k. \tag{24}$$

Equation (24) relates to $A(\mathbf{u})$ and to small differences $\Delta\mathbf{u}$ and $\Delta\mathbf{f}$. We now consider finite differences over discrete intervals (cells) and construct *average values*, $\tilde{\alpha}$, $\tilde{\lambda}$, $\tilde{\mathbf{e}}$, $\tilde{\rho}$ and $\tilde{v}$, which satisfy discrete versions of (9) to (24), at least to first order.

3.2.2 The Payne-Whitham Model

For the PW model, (23) gives

$$\begin{pmatrix} \Delta\rho \\ \Delta\rho v \end{pmatrix} = \alpha_1 \begin{pmatrix} 1 \\ \frac{\rho v}{\rho} + C_o \end{pmatrix} + \alpha_2 \begin{pmatrix} 1 \\ \frac{\rho v}{\rho} - C_o \end{pmatrix}. \tag{25}$$

Solving for α_1 and α_2, we get

$$\alpha_1 = \frac{1}{2}\Delta\rho + \frac{1}{2C_o}\left(\Delta(\rho v) - \frac{\rho v}{\rho}\Delta\rho\right) \tag{26}$$

and

$$\alpha_2 = \frac{1}{2}\Delta\rho - \frac{1}{2C_o}\left(\Delta(\rho v) - \frac{\rho v}{\rho}\Delta\rho\right). \tag{27}$$

The discrete averages are therefore

$$\tilde{\lambda}_k = \tilde{v} \pm C_o, \tag{28}$$

$$\tilde{\alpha}_k = \frac{1}{2}\Delta\rho \pm \frac{1}{2C_0}\left(\Delta(\rho v) - \tilde{v}\Delta\rho\right), \tag{29}$$

and

$$\tilde{\mathbf{e}}_k = \begin{bmatrix} 1 \\ \tilde{v} \pm C_o \end{bmatrix}. \tag{30}$$

Roe [15] showed that one way of satisfying

$$\Delta\mathbf{f} = \tilde{A}\Delta\mathbf{u} \tag{31}$$

for the PW model, is to define $\tilde{\rho}$ as

$$\tilde{\rho} = \sqrt{\rho_r \rho_l}, \tag{32}$$

ρ_r being ρ at the right end of the cell, and ρ_l being ρ at the left end of the cell. $\tilde{v}$ is then found from (24), requiring

$$\begin{aligned}\Delta f_2 = \Delta\left(\frac{(\rho v)^2}{\rho}\right) + \Delta\left(C_o^2\rho\right) &= \left(\tilde{v}^2 + C_o^2\right)(\tilde{\alpha}_1 + \tilde{\alpha}_2) + 2\tilde{v}C_o(\tilde{\alpha}_1 - \tilde{\alpha}_2) \\ &= \left(\tilde{v}^2 + C_o^2\right)\Delta\rho + 2\tilde{v}\left(\Delta(\rho v) - \tilde{v}\Delta\rho\right)\end{aligned}$$

to hold. This leads to

$$\tilde{v} = \frac{\left(\sqrt{\rho_r}v_r + \sqrt{\rho_l}v_l\right)}{\left(\sqrt{\rho_r} + \sqrt{\rho_l}\right)} \tag{33}$$

(see [4] for details).

3.2.3 The Aw-Rascle Model

We use (23) to find $\alpha_{1,2}$, where

$$\begin{pmatrix} \Delta\rho \\ \Delta y \end{pmatrix} = \alpha_1 \begin{pmatrix} 1 \\ v + (\gamma+1)P \end{pmatrix} + \alpha_2 \begin{pmatrix} 1 \\ v + P \end{pmatrix},$$

and hence the Roe averages $\tilde{\alpha}_{1,2}$, for the Aw-Rascle model are found in the same way as before. This gives us

$$\tilde{\alpha}_1 = \frac{\Delta y - (\tilde{v} + \tilde{P})\Delta\rho}{\gamma\tilde{P}},$$

$$\tilde{\alpha}_2 = \frac{\left(\tilde{v} + (\gamma+1)\tilde{P}\right)\Delta\rho - \Delta y}{\gamma\tilde{P}}.$$

Now we need to find the Roe averages $\tilde{v}$ and $\tilde{P}$. Using (31) we have that

$$\Delta(y - \rho P) = -(\gamma+1)\tilde{P}\Delta\rho + \Delta y, \tag{34}$$

and

$$\Delta\left(\frac{y^2}{\rho^2} - Py\right) = -\left(\tilde{v}^2 + (\gamma+2)\tilde{P}\tilde{v} + (\gamma+1)\tilde{P}^2\right)\Delta\rho + (2\tilde{v} + \tilde{P})\Delta y. \tag{35}$$

It is easily seen from (34) that

$$\tilde{P} = \frac{\Delta\rho P}{(\gamma+1)\Delta\rho} \tag{36}$$

satisfies (31). Finding Roe averages for $\tilde{v}$ from (35) involves rewriting (35) as

$$a\tilde{v}^2 + b\tilde{v} + c = 0 \tag{37}$$

where

$$a = \Delta\rho,$$
$$b = (\gamma + 2)\tilde{P}\Delta\rho - 2\Delta y,$$

and

$$c = \Delta\left(\frac{y^2}{\rho^2} - Py\right) + (\gamma + 1)\tilde{P}^2\Delta\rho - \tilde{P}\Delta y.$$

$\tilde{v}$ can then be found using the quatratic formula

$$\tilde{v} = \frac{2c}{-b \mp \sqrt{b^2 - 4ac}}. \tag{38}$$

The Roe averages in each cell must lie between the values at the nodes at either end of the cell. This decides which root to take for (38).

We are now ready to apply Roe's scheme.

3.3 Roe Decomposition with First Order Upwind

Once we have found the Roe averages we can implement the scheme component by component, in the same way as the First Order Upwind scheme (see [11]). The values at the new time step are equal to the old ones plus the addition of

$$\tilde{\psi}_k = -\frac{\Delta t}{\Delta x}\tilde{\lambda}_k\tilde{\alpha}_k\tilde{\mathbf{e}}_k \begin{cases} to \quad \mathbf{u}_{j+1} \quad if \quad \tilde{\lambda}_k > 0, \quad or \\ to \quad \mathbf{u}_j \quad if \quad \tilde{\lambda}_k < 0, \end{cases} \tag{39}$$

for k =1, 2.

3.4 Roe Decomposition with Second Order

A second step may be applied after First Order Upwind to give the scheme second order accuracy.

If $\tilde{\lambda}_k > 0$

$$\left.\begin{aligned} \mathbf{u}_j^n &\rightarrow \mathbf{u}_j^{n*} + \frac{1}{2}\left(1 - \tilde{\lambda}_k\frac{\Delta t}{\Delta x}\right)\tilde{\psi}_k, \\ \mathbf{u}_{j+1}^n &\rightarrow \mathbf{u}_{j+1}^{n*} - \frac{1}{2}\left(1 - \tilde{\lambda}_k\frac{\Delta t}{\Delta x}\right)\tilde{\psi}_k, \end{aligned}\right\} \tag{40}$$

else if $\tilde{\lambda}_k < 0$

$$\left.\begin{aligned} \mathbf{u}_j^n &\rightarrow \mathbf{u}_j^{n*} - \frac{1}{2}\left(1 - \tilde{\lambda}_k \frac{\Delta t}{\Delta x}\right)\tilde{\psi}_k, \\ \mathbf{u}_{j+1}^n &\rightarrow \mathbf{u}_{j+1}^{n*} + \frac{1}{2}\left(1 - \tilde{\lambda}_k \frac{\Delta t}{\Delta x}\right)\tilde{\psi}_k. \end{aligned}\right\} \tag{41}$$

Where $\mathbf{u}_j^{n*}$ is the solution $\mathbf{u}_j^n$ after First Order Upwind has been applied. For each separate k this is equivalent to the Lax-Wendroff scheme.

3.5 Use of Flux Limiters

One of the drawbacks of second order schemes is the appearance of oscillations. The second order step of a scheme overcompensates for the diffusive nature of a first order step. We therefore add an extra feature which is designed to prevent these oscillations, namely a Flux Limiter ϕ_j. The Minmod Flux Limiter replaces $\tilde{\psi}_k$ in the second step above. If the first components of

$$\tfrac{1}{2}\left(1 - \tilde{\lambda}_k \tfrac{\Delta t}{\Delta x}\right)\tilde{\psi}_k, \quad \tfrac{1}{2}\left(1 - \tilde{\lambda}_k \tfrac{\Delta t}{\Delta x}\right)\tilde{\psi}_{upwind}$$

are of opposite signs, then $\tilde{\phi}_k = 0$. If not, consider the absolute values. If the first components of

$$\left|\frac{1}{2}\left(1 - \tilde{\lambda}_k \frac{\Delta t}{\Delta x}\right)\tilde{\psi}_k\right| < \left|\frac{1}{2}\left(1 - \tilde{\lambda}_k \frac{\Delta t}{\Delta x}\right)\tilde{\psi}_{upwind}\right|$$

then $\tilde{\phi}_k = \tilde{\psi}_k$, otherwise $\tilde{\phi}_k = \tilde{\psi}_{upwind}$.

The second stage is then applied as with (40) and (41), but with $\tilde{\phi}_k$ replacing $\tilde{\psi}_k$.

So if $\tilde{\lambda}_k > 0$

$$\left.\begin{aligned} \mathbf{u}_j^n &\rightarrow \mathbf{u}_j^{n*} + \frac{1}{2}\left(1 - \tilde{\lambda}_k \frac{\Delta t}{\Delta x}\right)\tilde{\phi}_k, \\ \mathbf{u}_{j+1}^n &\rightarrow \mathbf{u}_{j+1}^{n*} - \frac{1}{2}\left(1 - \tilde{\lambda}_k \frac{\Delta t}{\Delta x}\right)\tilde{\phi}_k, \end{aligned}\right\} \tag{42}$$

else if $\tilde{\lambda}_k < 0$

$$\left.\begin{aligned} \mathbf{u}_j^n &\rightarrow \mathbf{u}_j^{n*} - \frac{1}{2}\left(1 - \tilde{\lambda}_k \frac{\Delta t}{\Delta x}\right)\tilde{\phi}_k, \\ \mathbf{u}_{j+1}^n &\rightarrow \mathbf{u}_{j+1}^{n*} + \frac{1}{2}\left(1 - \tilde{\lambda}_k \frac{\Delta t}{\Delta x}\right)\tilde{\phi}_k. \end{aligned}\right\} \tag{43}$$

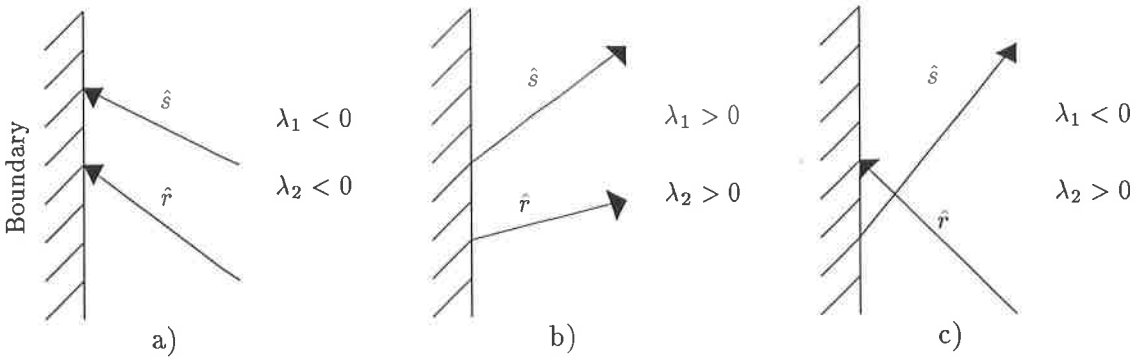

Figure 1: When to use boundary data.

3.6 Boundary Conditions and Riemann Invariants

The question remains of what to do at the boundaries. If both wave speeds $\lambda_{1,2}$ are of the same sign at the boundary, then the waves are either both going into, or both coming out of the boundary. If they are both going into the boundary then there is no need for boundary data (Fig.1a). Indeed, if boundary data was supplied the problem would be over prescribed. If both of the waves are coming out of the boundary, then we must impose both density and velocity from the M25 data supplied (Fig.1b). If the wave speeds are of opposite signs, however, then we only need to supply the data for the wave coming out of the boundary (see Fig.1c). This can be done by splitting the system up into its component waves.

Taking the system in the form of (8), having found the eigenvalues $\lambda_{1,2}$, and eigenvectors $\mathbf{e}_{1,2}$, we construct a matrix X whose columns are the eigenvectors of A together with a diagonal matrix Λ whose entries are the corresponding eigenvalues. Premultiplying (8) by X^{-1} and using $XX^{-1} = I$, we get

$$X^{-1}\mathbf{u}_t + X^{-1}AXX^{-1}\mathbf{u}_x = \mathbf{0}.$$

Substituting for $X^{-1}AX = \Lambda$ and equating

$$\hat{\mathbf{r}}_t = X^{-1}\mathbf{u}_t, \quad \hat{\mathbf{r}}_x = X^{-1}\mathbf{u}_x, \tag{44}$$

where

$$\hat{\mathbf{r}} = \begin{pmatrix} \hat{r} \\ \hat{s} \end{pmatrix},$$

we are able to integrate (44) and hence express $\hat{r}$ and $\hat{s}$ explicitly in terms of the conserved variables $\mathbf{u}$. Using this transformation, the system can therefore be expressed as

$$\hat{\mathbf{r}}_t + \Lambda \hat{\mathbf{r}}_x = \mathbf{0} \tag{45}$$

which has separated the system into two non-linear scalar advection equations in $\hat{r}$ and $\hat{s}$. These are called the Riemann Invariants as they are constant along the characteristics $dx/dt = \lambda_{1,2}$ respectively.

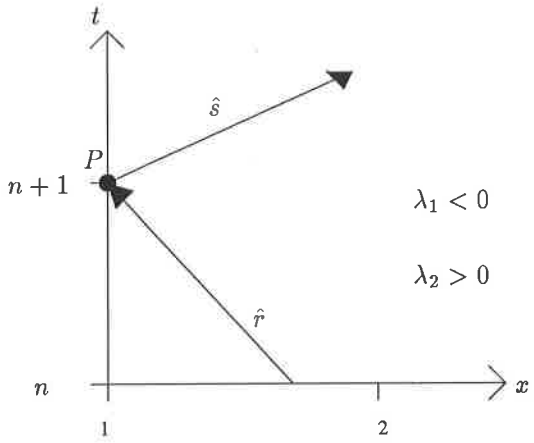

Figure 2: Deciding what data to use to calculate Riemann Invariants, depending on direction of flow of the two component waves.

Consider the case when $\lambda_1 < 0$ and $\lambda_2 > 0$ (Fig.(2)) at the left hand boundary, where the direction of flow is from left to right. $\hat{r}$ is coming into the boundary at P so is found by tracing back the characteristic to time n, into the cell between nodes 1 and 2. $\hat{s}$ is coming out of the boundary at P so is calculated from the collected M25 data. Once $\hat{r}$ and $\hat{s}$ are known we can calculate $\mathbf{u}^{n+1}$ at the point P by rearranging the solution found by integrating (44).

3.6.1 Riemann Invariants for the Payne-Whitham Model

Applying (44) and (45) to the Payne-Whitham model, we have that

$$X = \begin{pmatrix} 1 & 1 \\ v + C_0 & v - C_0 \end{pmatrix}, \quad X^{-1} = \frac{-1}{2C_0} \begin{pmatrix} v - C_0 & -1 \\ -(v + C_0) & 1 \end{pmatrix},$$

and

$$\Lambda = \begin{pmatrix} \lambda_1 & 0 \\ 0 & \lambda_2 \end{pmatrix} = \begin{pmatrix} v + C_0 & 0 \\ 0 & v - C_0 \end{pmatrix}.$$

From (44) we have that

$$\begin{aligned} \hat{r}_t &= -\frac{1}{2C_0}(v - C_0)\rho_t + \frac{1}{2C_0}(\rho v)_t \\ &= \frac{1}{2C_0}\left(C_0\rho_t + \rho v_t\right) \\ &= \frac{\rho}{2C_0}\left(v_t + C_0(ln\rho)_t\right), \end{aligned} \tag{46}$$

and similarly for $\hat{r}_x$. The partial differential equation for $\hat{s}$ is found to be

$$\hat{s}_t = -\frac{\rho}{2C_0}\left(v_t - C_0(ln\rho)_t\right). \tag{47}$$

Equations (46) and (47) cannot be solved explicitly. However we are looking for Riemann Invariants that satisfy (45). If we rewrite (46) and (47) as

$$\hat{\mathbf{r}}_t = M\mathbf{r}_t \tag{48}$$

where

$$M = \frac{\rho}{2C_0}\begin{pmatrix} 1 & 0 \\ 0 & -1 \end{pmatrix}$$

and

$$\mathbf{r} = \begin{pmatrix} r \\ s \end{pmatrix} = \begin{pmatrix} v + C_0 ln(\rho) \\ v - C_0 ln(\rho) \end{pmatrix}, \tag{49}$$

then substituting (48) into (45) we have that

$$M\left(\mathbf{r}_t + \Lambda\mathbf{r}_x\right) = \mathbf{0},$$

and provided $\rho \neq 0$ M is invertible, hence

$$\mathbf{r}_t + \Lambda\mathbf{r}_x = \mathbf{0},$$

and the components of $\mathbf{r}$ in (49) are the Riemann Invariants with wavespeeds $\lambda_{1,2}$ respectively.

Considering the case when $\lambda_1 < 0$ and $\lambda_2 > 0$ (Fig.2) we calculate r by tracing back the characteristic to the previous time step into the cell between nodes 1 and 2, and take a linear interpolation between $\mathbf{u}_1$ and $\mathbf{u}_2$ to find the corresponding $\mathbf{u}_I$. r is then calculated using $\mathbf{u}_I$ and s is calculated from the M25 data at time $n+1$, $\mathbf{u}_{M25}^{n+1}$, using (49). $\mathbf{u}^{n+1}$ is then calculated by rearranging (49), i.e.

$$\begin{aligned} v &= \frac{1}{2}(r+s), \\ \rho &= exp\left(\frac{r-s}{2C_0}\right). \end{aligned}$$

3.6.2 Riemann Invariants for the Aw-Rascle Model

For the Aw-Rascle model we have

$$X = \begin{pmatrix} 1 & 1 \\ v+(\gamma+1) & v+P \end{pmatrix}, \quad X^{-1} = \frac{-1}{\gamma P}\begin{pmatrix} v+P & -1 \\ -v-(\gamma+1)P & 1 \end{pmatrix}$$

and

$$\Lambda = \begin{pmatrix} v & 0 \\ 0 & v-\gamma P \end{pmatrix},$$

constructed from the eigenvalues and eigenvectors of A.

From (44), we have that

$$\begin{aligned} \hat{r}_t &= -\frac{-1}{\gamma P}\left((v+P)\rho_t - y_t\right) \\ &= \frac{-1}{\gamma P}\left(-\rho v_t - \gamma P \rho_t\right) \\ &= \frac{\rho}{\gamma P}\left(v_t + P_t\right), \end{aligned} \tag{50}$$

and similarly for $\hat{r}_x$. The partial differential equation for $\hat{s}$ is found to be

$$\begin{aligned} \hat{s}_t &= \frac{-1}{\gamma P}\left(\left(-v-(\gamma+1)P\right)\rho_t + y_t\right), \\ &= \frac{-\rho}{\gamma P} v_t. \end{aligned} \tag{51}$$

Again, (50) and (51) cannot be solved explicitly, so we rewrite them as (48) where

$$M = \frac{\rho}{\gamma P}\begin{pmatrix} 1 & 0 \\ 0 & -1 \end{pmatrix}$$

and

$$\mathbf{r} = \begin{pmatrix} r \\ s \end{pmatrix} = \begin{pmatrix} v + P \\ v \end{pmatrix}, \tag{52}$$

then substituting (48) into (45) we have that

$$M\left(\mathbf{r}_t + \Lambda \mathbf{r}_x\right) = \mathbf{0},$$

and provided $\frac{\rho}{\gamma P} \neq 0$, and hence $\rho \neq 0$, M is invertible, therefore

$$\mathbf{r}_t + \Lambda \mathbf{r}_x = \mathbf{0},$$

and the components of $\mathbf{r}$ in (52) are the Riemann Invariants with wavespeeds $\lambda_{1,2}$ respectively.

Again, if we consider the case when $\lambda_1 < 0$ and $\lambda_2 > 0$ (Fig.2) we calculate r by tracing back the characteristic to the previous time step into the cell between nodes 1 and 2, and take a linear interpolation between $\mathbf{u}_1$ and $\mathbf{u}_2$ to find the corresponding $\mathbf{u}_I$. r is then calculated using $\mathbf{u}_I$ and s is calculated from the M25 data at time $n+1$, $\mathbf{u}_{M25}^{n+1}$, using (52). Again, $\mathbf{u}^{n+1}$ is calculated by rearranging (52) to get

$$\rho = e^{\left(\frac{r-s}{2C_0}\right)},$$

$$v = \frac{1}{2}(r+s).$$

4 Results

The Lax-Friedrichs scheme was compared to the first and second order upwind schemes. They all gave similar behaviour, but as expected the Lax-Friedrichs was the most diffusive. The second order scheme with flux limiters gave the least diffusive results, hence it is this scheme that is plotted in Fig. 3.

The solid line is the representation of the collected data from the M25 motorway. To make the comparison as fair as possible the M25 has no on/off

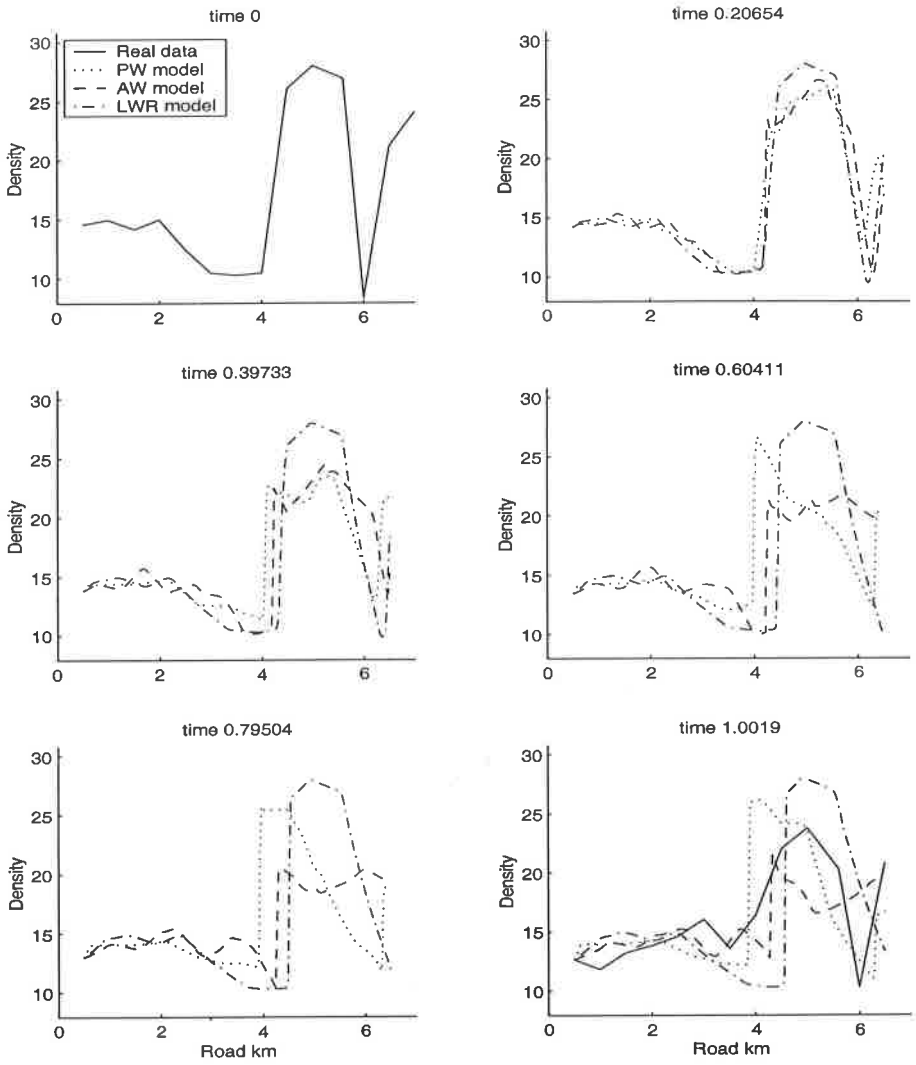

Figure 3: Comparison of the PW, AR and LWR models using second order scheme with flux limiters. $Co = 90$ for the PW model, $\gamma = 1.4$ for the AR model and f_2 is the flux function used for the LWR model. Time is in minutes.

ramps along the section we are considering, since the model in its present form doesn't allow for them. The data is collected at one-minute intervals, and Fig. 3 is taken from the data at 15/07/99 at 09:30. See [11] for details of how the data was averaged over the four lanes. The averaged data has waves of variations in density moving at constant speed, both in the positive direction and in the negative direction against the flow. Fig. 3 shows the larger peak of density approximately 27 veh/km moving slowly with the flow of traffic and decreasing gradually in height. There is a stationary trough at approximately 6 km from the first post, and some smaller peaks moving in the positive direction starting from approximately 1 and 2 km from the first post, moving with faster speed than the larger peak. These are some of the features we would like to mimic.

For the PW model the constant value C_0 was taken to be 90. This seemed to produce the most realistic results for this set of data. The model preserved the larger peak and trough, but not quite at the correct speeds, and the shapes were distorted. The smaller peaks were not modelled particularly well though.

The constant value of γ for the AR model was taken to be 1.4. This model also preserved the larger peak at roughly the correct speed, but again the shape was distorted. The trough however had too large a wavespeed and was soon lost out of the boundary. The smaller peaks were modelled with more accuracy, although the waves were a little slow.

The Lighthill-Whitham-Richards model discussed in [11] has also been included to show how it compares to the two-equation models discussed in this paper. The flux function chosen for this comparison was $f_2 = \rho V_2(\rho)$ where

$$V_2(\rho) = U_{max} exp^{-9\rho/\rho_{max}}.$$

U_{max} is some maximum speed of the road and ρ_{max} is some maximum density. Again, it preserves the larger peak and shows the least distortion of the shape and has the closest wave speed to the real data. It fares less well however with smaller density flow.

5 Conclusions

Both the PW and AR models were able to capture the movement of certain features but were unable to preserve the shape of the larger peak. They were also unable to capture the movement of both the trough and the smaller peaks. Neither model gave satisfactory results overall, so more work is needed to try to make them more realistic.

6 Further Work

6.1 Reduction of the Payne-Whitham Model

Here we obtain a first order approximation to $V(\rho)$ from the second equation of the PW model and substitute it back into the first equation. This reduces the system down to a one equation model with features from the two equation model. We intend to apply numerical schemes to this and compare the results to other models and the M25 data.

6.2 Use of relaxation terms in both models

Relaxation terms can be added to both models to incorporate the driver's behaviour. The use of these terms makes the application of conservative schemes more of a challenge, but could make the models more realistic.

6.3 Linear Combination of the Payne-Whitham and Aw-Rascle models

In order to try to capture some of the best features of both the PW and AR models, a linear combination of them could be considered. The first equation (1) is common to both, so that is kept as it is. The second equation is (5) (with zero rhs) multiplied by θ added to (16) multiplied by $(1-\theta)$, where $0 \leq \theta \leq 1$. This gives the system

$$(\rho)_t + (\rho v)_x = 0,$$

$$(\theta\rho v + (1-\theta)\,\rho\,(v+P))_t + \left(\theta\left(\frac{(\rho v)^2}{\rho} + C_0^2\rho\right) + (1-\theta)\,\rho v\,(v+P)\right)_x = 0$$

This can then be discretised and the results compared to the real data.

6.4 Use of Dafermos Method

It has been suggested that the characteristic-based numerical scheme of Dafermos [3] would be very suitable for this type of problem. This will be investigated further.

Aknowledgements

This research is supported by the E.P.S.R.C. and supervised by Prof. Mike Baines and Dr. Pete Sweby from the University of Reading. I would also like to thank Jo White from TRL for useful discussions and the Highways Agency, in particular Brian Harbord from TSS Division, for the traffic data analysed in this report.

References

[1] A.Aw and M.Rascle. *Resurrection of 'second order' models of traffic flow?* SIAM J. Appl. Math., 60, pp 916-938 (2000).

[2] C.Daganzo. *Requiem for second-order fluid approximations of traffic flow.* Transpn. Res.-B 29B, pp 277-286 (1995).

[3] C.M.Dafermos. *Polygonal approximations of solutions of the initial-value problem for a conservation law.* J. Math. Anal. Appl., 38, pp 33-41 (1972).

[4] P.Glaister. *Difference Schemes For The Shallow Water Equations.* Numerical Analysis Report 9/87, Dept. of Mathematics, University of Reading (1987).

[5] D.Helbing. *Gas-kinetic derivation of Navier-Stokes-like traffic equations* Phys Rev E, 53, pp 2366-2381 (1996).

[6] B.S.Kerner and P.Konhäuser. *Cluster effects in initially homogeneous traffic flow.* Phys Rev E, 48, pp R2335-R2338 (1993).

[7] B.S.Kerner and P.Konhäuser. *Structure and parameters of clusters in traffic flow.* Phys Rev E, 50, pp 54-83 (1994).

[8] B.S.Kerner, P.Konhäuser, and M.Schilke. *Deterministic spontaneous appearance of traffic jams in slightly inhomogeneous traffic flow.* Phys Rev E, 51, pp 6243-6246 (1995).

[9] R.J.LeVeque. *Numerical Methods for Conservation Laws.* Birkhäuser (1992).

[10] M.J.Lighthill and G.B.Whitham. *On kinematic waves. I:Flow movement in long rivers. II:A Theory of traffic flow on long crowded roads.* Proc. Royal Soc., A229, pp 281-345 (1955).

[11] J.V.Morgan *Numerical Modelling of Traffic on the M25 Motorway: Part I* Numerical Analysis Report 2/2001, Dept. of Mathematics, University of Reading (2001).

[12] K.Nagel. *Particle hopping models and traffic flow theory.* Phys Rev E, 53, pp 4655-4672 (1986).

[13] H.J.Payne. *Models of freeway traffic and control.* Math.Models Publ. Sys.Simul. Council Proc.,28, pp 51-61 (1971).

[14] P.I.Richards. *Shockwaves on the highway.* Operations Research, 4, pp 42-51 (1956).

[15] P.L.Roe *Approximate Riemann Solvers, parameter vectors, and difference schemes.* Journal of Computational Physics vol.43 pp 357-372, (1981).

[16] P.K.Sweby. *High Resolution Schemes Using Flux Limiters For Hyperbolic Conservation Laws.* SIAM J. Numer. Anal. 21, pp 995-1011 (1984).

[17] G.B.Whitham. *Linear and Nonlinear Waves.* John Wiley, New York, (1974).